UNITED STATES DEPARTMENT OF THE INTERIOR

GEOLOGICAL SURVEY

Particle Motion Inside a Fluid-Filled Borehole From Incident Plane Waves

By M. W. Lee[1]

Open-File Report 85-734

[1]U.S. Geological Survey, Box 25046, Denver Federal Center, Denver, Colorado 80225

1985

CONTENTS

ILLUSTRATIONS

PARTICLE MOTION INSIDE A FLUID-FILLED BOREHOLE FROM INCIDENT PLANE WAVES

By M. W. Lee

ABSTRACT

The particle motions inside a fluid-filled borehole from incident plane waves were studied under the assumption that the wavelength of the incident wave is very large compared to the borehole diameter. These particle motions were formulated by applying the continuity of the radial displacement boundary condition to the particle motion at the wall of the fluid-filled borehole as derived by Lee (1985a). This study shows that incident plane waves generate not only axis-symmetrical pressure but also axis-asymmetrical pressure which approaches zero as borehole diameter approaches zero.

INTRODUCTION

The particle motion induced in the surrounding earth medium from the seismic wave is the most important information acquired by the vertical seismic profiling (VSP) method and is recorded by a wall-locking geophone. Sometimes the fluid motion inside a borehole is measured by a suspended hydrophone or geophone for a particular purpose desired for the VSP method. For example, Huang and Hunter (1981) showed the importance of the fluid pressure in detecting open fractures in the rock. Thus, fluid motion inside a borehole from incident plane waves is the principle focus of this paper.

White (1965) formulated pressure response in the borehole fluid for the incident P- and SV-waves by summation of elementary pressure caused by the traveling wave and showed that the fluid motion is axis-symmetrical in the low-frequency limit. In this paper, the particle motions in the borehole fluid were formulated by applying one of the boundary conditions at the wall of the borehole (which is the continuity of the radial displacement) to the displacement in the surrounding solid from the incident plane waves as derived by Lee (1985a). The displacement fields of Lee (1985a) were derived under the assumption that the wavelength of interest is very large compared to the borehole diameter. This paper, in addition to the study by Lee (1985a), completes the investigation of particle motion in and on the fluid-filled borehole from incident plane waves.

By retaining terms proportional up to second-order frequency, the borehole fluid pressure from the incident P- or SV-wave is shown to consist of an axis-symmetrical component (which is finite as the borehole diameter approaches zero) and an axis-asymmetrical component (which approaches zero as borehole diameter approaches zero). On the other hand, the incident SH-wave generates only axis-asymmetrical pressure inside the fluid-filled borehole.

DERIVATION OF PARTICLE MOTION

Assuming that a cylindrical borehole with a radius "a" is embedded in an isotropic, homogeneous, elastic medium with P-wave velocity α, S-wave velocity β, and density ρ, the fluid inside the borehole has a compressional velocity α_f and density β_f. The particle displacement potential inside a fluid-filled borehole (Φ) can be written in the frequency domain (Lee, 1985a) as:

$$\Phi = \sum_{p=-\infty}^{\infty} \int_{-\infty}^{\infty} D_p J_p(\ell r) e^{-ikz} e^{ip\theta} dk, \tag{1}$$

where D_p is the unknown constant to be determined, J_p is the Bessel function of the p-th order, and ℓ is radial wavenumber which is given by

$$\ell = \left(\frac{\omega^2}{\alpha_f^2} - k^2 \right)^{1/2}.$$

Equation (1) satisfies the following wave equation:

$$\nabla^2 \Phi = -\omega^2 \Phi / \alpha_f^2. \tag{2}$$

The particle displacement field U_r, U_Θ, and U_z, and pressure P can be written in a cylindrical coordinate system (fig. 1) as:

$$U_r = \frac{\partial \Phi}{\partial r},$$

$$U_\theta = \frac{1}{r} \frac{\partial \Phi}{\partial \theta}, \tag{3}$$

$$U_z = \frac{\partial \Phi}{\partial z},$$

and

$$P = \rho_f \omega^2 \Phi.$$

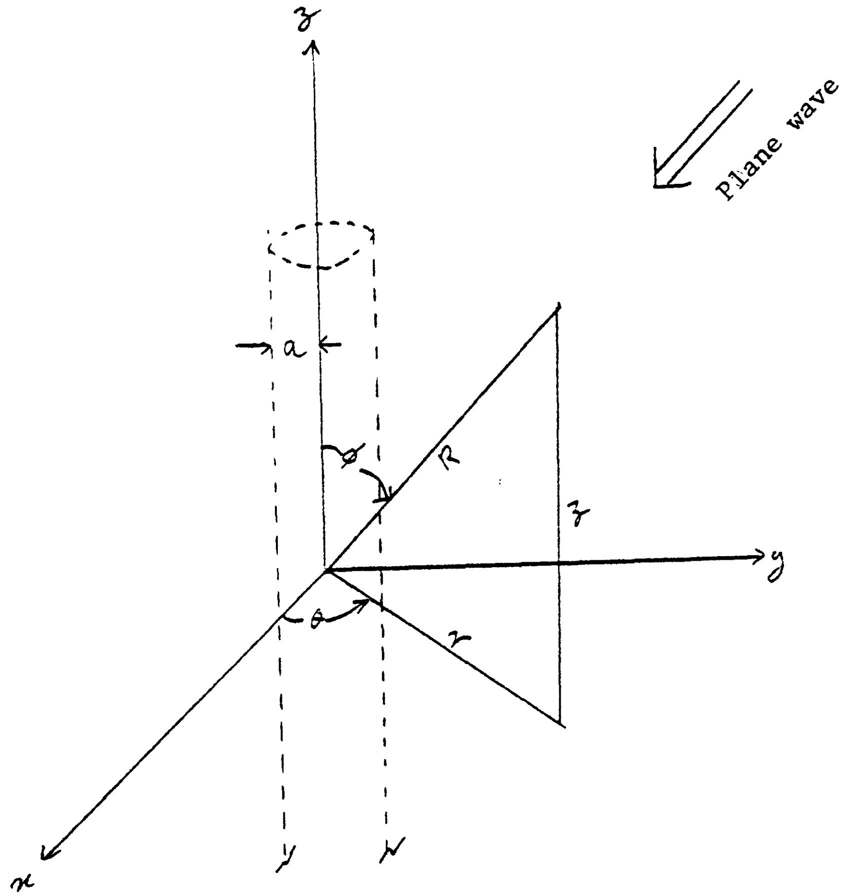

Figure 1.--Coordinate system for the analysis. An orthogonal Cartesian coordinate system (x, y, z), a cylindrical coordinate system (r, θ, z), and a spherical coordinate system (R, Ø, θ) are shown. Incident angles of plane waves are given by Ø.

The general approach to solve equation (2) for the incident plane waves requires a great deal of complicated mathematics including the plane-wave decomposition into cylindrical waves. In this paper, the known displacement fields at the wall of a fluid-filled borehole for the incident plane waves and the boundary condition of the continuity of the radial displacement were utilized in order to solve equation (2) under the assumption that the wavelength of interest is much larger than the borehole diameter.

The plane-wave solution of equation (1) can be written for the incident P-wave as:

$$\Phi = \sum_{p=-\infty}^{\infty} \int_{-\infty}^{\infty} D_p J_p(\ell r) e^{-ikz} e^{ip\theta} \delta(k \pm k_\alpha \cos\phi)\, dk, \tag{4}$$

and for the incident S-wave as:

$$\Phi = \sum_{p=-\infty}^{\infty} \int_{-\infty}^{\infty} D_p J_p(\ell r) e^{-ikz} e^{ip\theta} \delta(k \pm k_\beta \cos\phi)\, dk, \tag{5}$$

where δ is the Dirac delta function, $k_\alpha = \omega/\alpha$, $k_\beta = \omega/\beta$, and $\emptyset$ is the propagation angle of the incident plane wave with respect to the z-axis. Notice that $k_\alpha \cos\emptyset$ or $k_\beta \cos\emptyset$ represents the vertical wave number of the incident plane waves. Considering only the incoming plane waves (fig. 1), the solution (4) can be written as:

$$\Phi = \sum_{p=-\infty}^{\infty} \tilde{D}_p J_p(\tilde{\ell} r) e^{ik_\alpha \cos\phi} e^{ip\theta}, \tag{6}$$

where $\sim$ indicates the quantity substituted k by $k_\alpha \cos\emptyset$.

Thus the radial displacement at r = a, which is at the wall of the borehole, and z = 0 can be expressed [utilizing equations (3) and (6)] as:

$$U_r = \sum_{p=-\infty}^{\infty} \tilde{D}_p (-\tilde{\ell}) J_{p+1}(\tilde{\ell} r) e^{ip\theta}. \tag{7}$$

The boundary condition requires that the radial displacement U_r in the fluid should be equal to the radial displacement U_r in the solid at r = a. If the radial displacement at r = a in the solid is known, the unknown constant D_p can be evaluated by equating the two radial displacements.

Lee (1985a) derived the required displacement fields in the surrounding solid for incident plane waves using the seismic reciprocity theorem (see Appendix).

A. Incident P-wave.--By using equations (3), (7), and (A-1) shown in the appendix, and retaining the dominant terms of the Bessel function, the following equations can be derived.

$$
\begin{aligned}
&-\tilde{D}_0 \frac{\tilde{\ell} a}{2} + \tilde{D}_1 \tilde{\ell} \cos\theta + \tilde{D}_2 \frac{\tilde{\ell}^2 a}{2} \cos 2\theta \\
&\quad = S(\omega) \frac{i\omega a}{\alpha} \frac{\alpha^2 T_\alpha (1 - 2\beta^2 \cos^2\phi / \alpha^2)}{2\beta^2 (T_\alpha + \rho_f/\rho)} \\
&\quad + S(\omega) \sin\phi \cos\theta \\
&\quad + S(\omega) \frac{i\omega a}{\alpha} \frac{\sin^2\phi}{(1 - \beta^2/\alpha^2)} \cos 2\theta ,
\end{aligned}
\tag{8}
$$

where

$$
T_\alpha = \frac{\beta^2}{\alpha_f^2} \left(1 - \frac{\alpha_f^2 \cos^2\phi}{\alpha^2}\right) ,
$$

$$
\tilde{\ell} = \left(\frac{\omega^2}{\alpha_f^2} - k_\alpha^2 \cos^2\phi\right)^{1/2} .
$$

Therefore, the unknown quantity $\tilde{D}_p$ is written as:

$$
\begin{aligned}
\tilde{D}_0 &= \frac{-i\alpha S(\omega)}{\omega} \frac{(1 - 2\beta^2 \cos^2\phi / \alpha^2)}{(T_\alpha + \rho_f/\rho)} , \\
\tilde{D}_1 &= \frac{S(\omega)}{\tilde{\ell}} \sin\phi , \\
\tilde{D}_2 &= \frac{2i\omega S(\omega)}{\alpha \tilde{\ell}^2} \frac{\sin^2\phi}{(1 - \beta^2/\alpha^2)} .
\end{aligned}
\tag{9}
$$

Substituting equation (9) into equation (3), the particle displacements and pressure are expressed as:

$$U_r = S(\omega)\cos\theta\sin\phi + \frac{S(\omega)\, i\omega r}{\alpha}\left[\frac{\alpha^2 T_\alpha (1-2\beta^2\cos^2\phi/\alpha^2)}{2\beta^2 (T_\alpha + \rho_f/\rho)} + \frac{\cos 2\theta \sin^2\phi}{(1-\beta^2/\alpha^2)}\right],$$

$$U_\theta = -S(\omega)\left[\sin\theta\sin\phi + \frac{\sin 2\theta \sin^2\phi}{(1-\beta^2/\alpha^2)}\right], \tag{10}$$

$$U_z = S(\omega)\left[\frac{\cos\phi\,(1-2\beta^2\cos^2\phi/\alpha^2)}{(T_\alpha + \rho_f/\rho)} + \frac{i\omega r\cos\theta\sin 2\phi}{2\alpha}\right],$$

and

$$p = -iS(\omega)\,\alpha\omega\rho_f\left[\frac{(1-2\beta^2\cos^2\phi/\alpha^2)}{(T_\alpha + \rho_f/\rho)} + \frac{i\omega r\cos\theta\sin\phi}{\alpha}\right].$$

B. Incident SV-wave.--By using equations (3), (7), and (A-2) in the appendix, and following the exact procedure for the incident P-wave, the following constant can be derived.

$$\tilde{D}_0 = -\frac{iS(\omega)}{\omega}\,\frac{\beta\sin 2\phi}{(T_\beta + \rho_f/\rho)},$$

$$\tilde{D}_1 = \frac{S(\omega)}{\tilde{\ell}}\cos\phi, \tag{11}$$

$$\tilde{D}_2 = \frac{iS(\omega)\,\omega}{\tilde{\ell}^2}\,\frac{\sin 2\phi}{\beta(1-\beta^2/\alpha^2)},$$

with

$$T_\beta = \frac{\beta^2}{\alpha_f^2}\left(1 - \frac{\alpha_f^2 \cos^2\phi}{\beta^2}\right)$$

$$\tilde{\ell} = \left(\omega^2/\alpha_f^2 - k_\beta^2 \cos^2\phi\right)^{1/2}.$$

The displacement field and pressure are

$$U_r = S(\omega)\cos\theta\cos\phi + S(\omega)\frac{i\omega r}{\beta}\left[\frac{T_\beta \sin 2\phi}{2\,(T_\beta + \rho_f/\rho)} + \frac{\cos 2\theta \sin 2\phi}{2\,(1-\beta^2/\alpha^2)}\right], \tag{12}$$

$$U_\theta = -S(\omega)\left[\sin\theta\cos\phi + \frac{i\omega r}{\beta}\,\frac{\sin 2\theta \sin 2\phi}{2\,(1-\beta^2/\alpha^2)}\right],$$

$$U_z = S(\omega)\left[\frac{\cos\phi \sin 2\phi}{(T_\beta + \rho_f/\rho)} + \frac{i\omega r}{\beta}\cos\theta\cos^2\phi\right],$$

and

$$p = -iS(\omega)\beta\omega\rho_f\left[\frac{\sin 2\phi}{(T_\beta + \rho_f/\rho)} + \frac{i\omega r}{\beta}\cos\theta\cos\phi\right].$$

C. Incident SH-wave.--The constants are:

$$\tilde{D}_0 = 0 \,,$$

$$\tilde{D}_1 = \frac{S(\omega)}{\tilde{\ell}} \,, \qquad (13)$$

$$\tilde{D}_2 = \frac{2i\omega \sin\phi}{\tilde{\ell}^2 \beta\,(1-\beta^2/\alpha^2)} \,.$$

The particle displacement and pressure for the incident SH-wave are:

$$U_r = S(\omega)\left[\sin\theta + \frac{i\omega r}{\beta}\,\frac{\sin 2\theta \sin\phi}{(1-\beta^2/\alpha^2)}\right],$$

$$U_\theta = S(\omega)\left[\cos\theta + \frac{i\omega r}{\beta}\,\frac{\cos 2\theta \sin\phi}{(1-\beta^2/\alpha^2)}\right], \qquad (14)$$

$$U_z = S(\omega)\,\frac{i\omega r}{\beta}\,\sin\theta\cos\phi \,,$$

and

$$p = -iS(\omega)\,\beta\omega\rho_f\,\frac{i\omega r}{\beta}\,\cos\theta \,.$$

DISCUSSION

The vertical component of the particle motion and pressure inside a fluid-filled borehole are the main quantities of interest in the VSP. The relation between the vertical component of particle displacement (U_z) and pressure (P) is given by:

$$P = \frac{-i \rho_f \omega \alpha}{\cos \phi} U_z . \tag{15}$$

Because the behavior of U_z can be inferred from that of the pressure, this section focuses on the discussion of pressure inside a fluid-filled borehole due to incident plane waves.

The pressure inside the borehole due to incident P- and SV-waves can be decomposed into two components: (1) the first-order or axis-symmetric component, a term proportional to the first power of frequency ω; and (2) the second-order or axis-asymmetric component, a term proportional to the second power of frequency. The first-order term is identical to the formula derived by White (1965). However, in the incident SH-wave, there is no axis-symmetrical motion inside a fluid-filled borehole except for the axis-asymmetrical motion. As shown in the equations, the fluid inside the borehole affects only the axis-symmetrical motion. The effect of the fluid on the axis-symmetrical motion can be analyzed by introducing tube-wave velocity (C_T) into the equation:

$$\frac{1 - 2\beta^2 \cos^2\phi / \alpha^2}{T_\alpha + \rho_f/\rho} \longrightarrow \frac{C_T^2}{\beta^2} \frac{1 - 2\beta^2 \cos^2\phi/\alpha^2}{(1 - C_T^2 \cos^2\phi/\alpha^2)} , \tag{16}$$

$$\frac{\sin 2\phi}{T_\beta + \rho_f/\rho} \longrightarrow \frac{C_T^2}{\beta^2} \frac{\sin 2\phi}{(1 - C_T^2 \cos^2\phi/\beta^2)} .$$

Figure 2 shows the quantities of equation (16) with respect to the incident angle ϕ and velocity ratio C_T/β. The solid line represents the first term of equation (16), which is for the incident P-wave, and the dotted line, for the incident SV-wave. This figure indicates that the contribution of the symmetrical component increases as the shear-wave velocity approaches the tube-wave velocity, and the effect of the fluid on pressure is very substantial. The maximum fluid pressure for the incident P-wave occurs at $\phi = 90^\circ$ and monotonically decreases with the decreasing angle of incidence. Peak pressure for the incident SV-wave occurs at:

$$\phi = \cos^{-1}\left[\sqrt{\frac{1}{1 - C_T^2/\beta^2}}\right]$$

and pressure decreases monotonically to zero at $\phi = 0^\circ$ and $\phi = 90^\circ$.

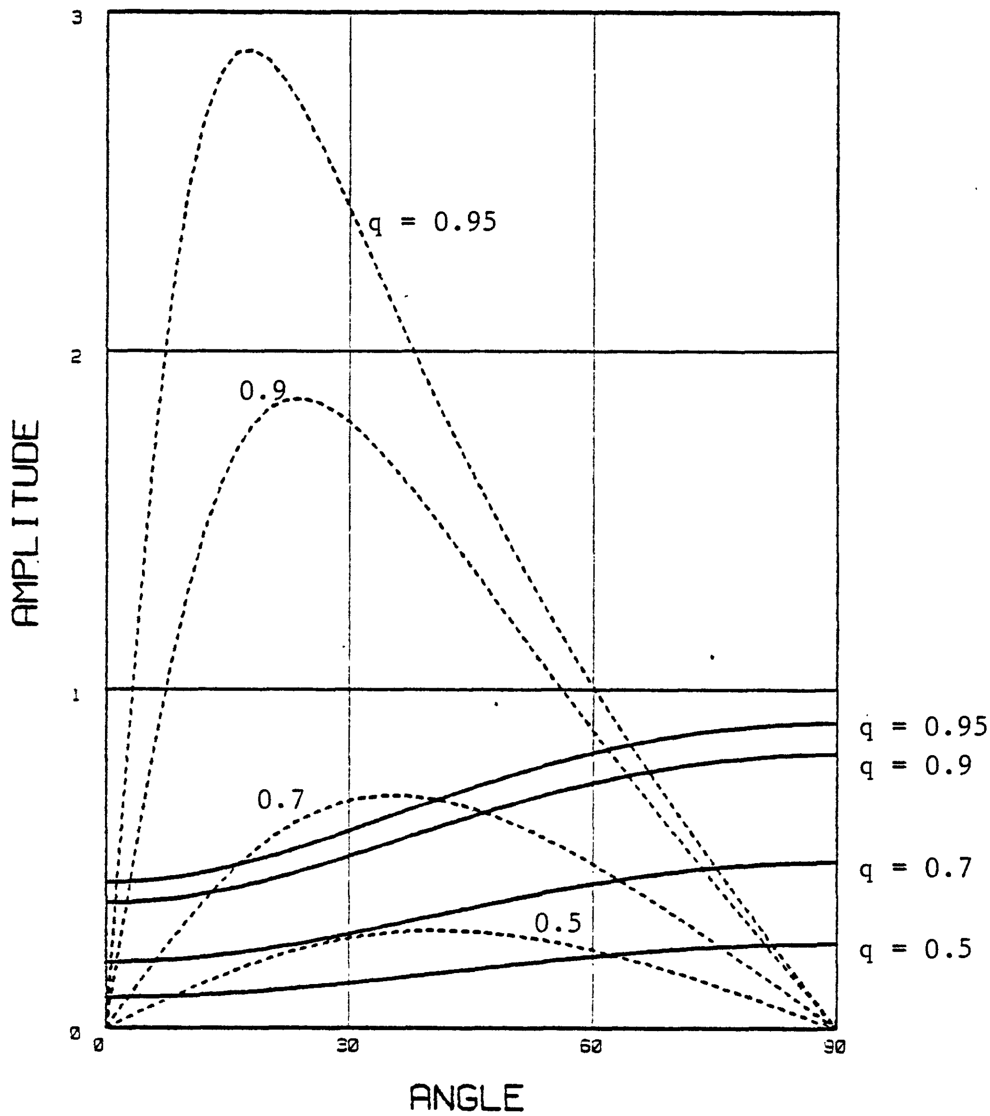

Figure 2.--The effect of fluid on the first-order pressure response (axis-symmetrical component) for the incident P-wave (heavy solid line) and for the SV-wave (heavy dotted line), with respect to the incident angle Ø and velocity ratio $q = C_T/\beta$.

The second-order term has maximum value at the wall of the borehole, r = a, and its contribution to the total pressure can be examined by the following transfer function concept defined as:

$$\text{Transfer function} \triangleq \frac{\text{total pressure}}{\text{symmetrical component of pressure.}}$$

For example, in the case of the incident P-wave, the transfer function T_p at r = a can be written as:

$$T_p \triangleq \left[1 + \frac{\omega^2 a^2 (T_\alpha + \rho_f/\rho)^2 \sin^2\phi \cos^2\theta}{\alpha^2 (1 - 2\beta^2 \cos^2\phi/\alpha^2)^2} \right]^{1/2} e^{i\phi_p} \tag{17}$$

with

$$\phi_p = \tan^{-1}\left[\frac{\omega a (T_\alpha + \rho_f/\rho) \sin\phi \cos\theta}{\alpha (1 - 2\beta^2 \cos^2\phi/\alpha^2)} \right]$$

$$\simeq \frac{\omega a (T_\alpha + \rho_f/\rho) \sin\phi \cos\theta}{\alpha (1 - 2\beta^2 \cos^2\phi/\alpha^2)} \qquad \text{when } \frac{\omega a}{\alpha} \ll 1 .$$

Figure 3 shows the transfer function for the incident P-wave with $\emptyset$ = 90^o, $\theta = 0^o$, ρ/ρ_f = 2.5, and α_f = 1,500 m/s with respect to the dimensionless parameter $2a/\lambda$, where λ is the wavelength and formation P-wave velocity α. When $2a/\lambda$ = 0.03, and α = 6,000 m/s, the amplitude of the total pressure increases about 15 percent and the phase advances about 15 degrees compared to the axis-symmetrical component; when $2a/\lambda$ = 0.03 and α = 2,000 m/s, the contribution of the second-order term is negligible. As shown in the figure, the contribution of the second-order term increases with increasing formation velocity simply because the contribution of the first-order term decreases with the increasing formation velocity. For the conventional near-offset VSP, the contribution of the second-order term is negligible as evidenced by equation (17).

The effect of the second-order component can be easily illustrated by the time-domain representation of the pressure. Figure 4 shows the pressure response for the incident P-wave using 250 Hz Ricker wavelet with $\emptyset$ = 90^o, θ = 0^o, ρ/ρ_f = 2.5, and α_f = 1,500 m/s. In this figure, the heavy solid line represents the first-order component; the light solid line, the second-order component; and the light dotted line, the total pressure. Figure 4a shows the pressure response for α = 4,000 m/s and a = 0.16 m, which is equivalent to $2a/\lambda_p$ = 0.02, where λ_p is the dominent wavelength. In this case, the second-order component is negligible compared to the first-order component.

Figure 4b shows the pressure response for α = 8,000 m/s and a = 0.032 m, which is also $2a/\lambda_p$ = 0.02. In this case, the contribution of the second-order component is substantial.

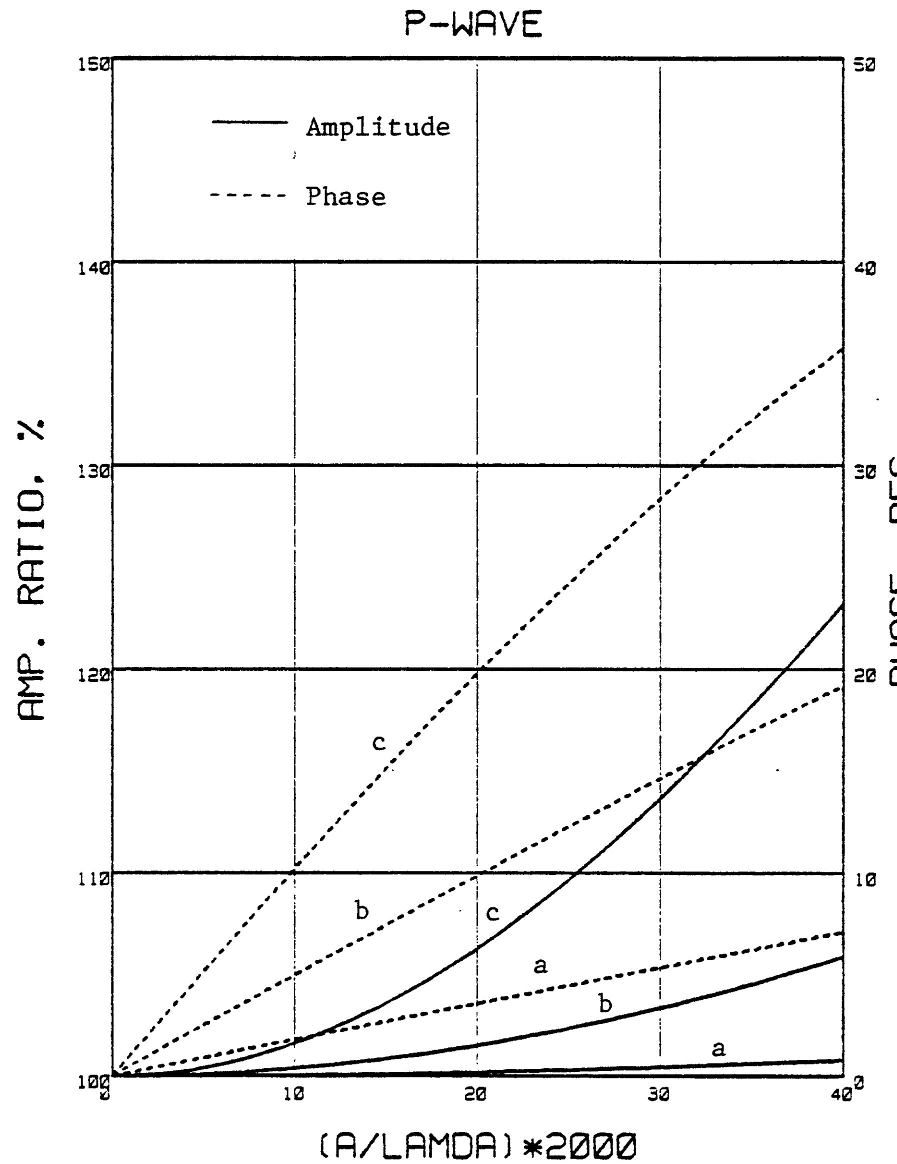

Figure 3.--Transfer function for the incident P-wave with respect to the dimensionless parameter $2a/\lambda$ and the formation of P-wave velocity with $\emptyset = 90^o$, $\theta = 0^o$, $r = a$, $\alpha_f = 1{,}500$ m/s, and $\rho/\rho_f = 2.5$. a) $\alpha = 2{,}000$ m/s; b) $\alpha = 4{,}000$ m/s; c) $\alpha = 6{,}000$ m/s.

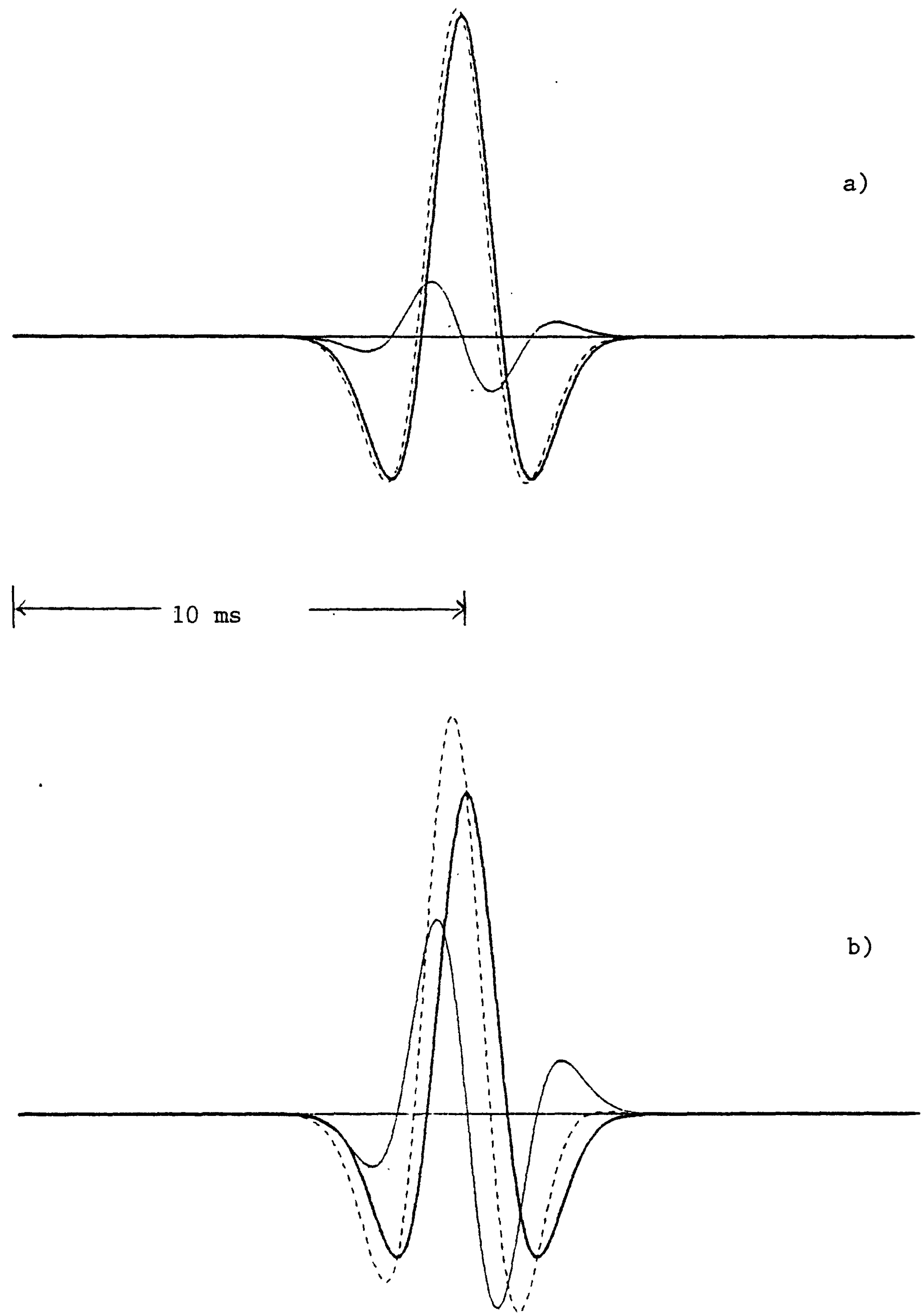

Figure 4.--Pressure response at $\theta = 0^{o}$ and $r = a$ using 250 Hz Ricker wavelet for the incident P-wave with respect to the formation of P-wave velocity with $\emptyset = 90^{o}$, $\alpha_f = 1{,}500$ m/s, and $\rho/\rho_f = 2.5$.

Heavy solid line represents the axis-symmetrical component; light solid line, the second-order component; and light dotted line, the total pressure. a) $\alpha = 4{,}000$ m/s and $a = 0.16$ m; b) $\alpha = 8{,}000$ m/s and $a = 0.32$ m.

When $\omega a/\alpha << 1$, the phase spectrum shown in equation (17) can be approximated in the time domain by $\delta(t + \tau)$, where

$$\tau = \frac{a(T_\alpha + \rho_f/\rho) \sin\phi \cos\theta}{\alpha(1 - 2\beta^2 \cos^2\phi/\alpha^2)} . \tag{18}$$

The effect of the phase shift due to the second-order component can be explained using the result shown in figure 5. In figure 5, the heavy solid line represents the pressure at r = 0, which is equivalent to the first-order component; the light solid line, at $\theta = 0^\circ$ and r = a; and the light dotted line, at $\theta = 180^\circ$ and r = a. About 0.4 ms arrival-time difference can be observed between the two azimuthal angles in this figure, which is very close to the predicted value 0.5 ms from equation (18).

Similar analyses can be performed for the incident SV-wave, and some of the examples are shown in figures 6 through 8. The results for the incident SV-wave are similar to those for the incident P-wave, except that the fluid has more pronounced effect.

REFERENCES CITED

Huang, C. F., and Hunter, J. A. M., 1981, The correlation of "tube wave" events with open fractures in fluid-filled boreholes, in current research, Part A: Paper 81-1A: Geological Survey of Canada, p. 161-376.

Lee, M. W., 1985a, Scattered waves on the wall of a fluid-filled borehole from incident plane waves: U.S. Geological Survey Open-File Report 85-666, 25 p.

______1985b, Two- and three-dimensional low-frequency radiation from an arbitrary source in a fluid-filled borehole: U.S. Geological Survey Open-File Report 85-550, 35 p.

White, J. E., 1965, Seismic waves: Radiation, transmission and attenuation: New York, McGraw-Hill Book Co., Inc., 302 p.

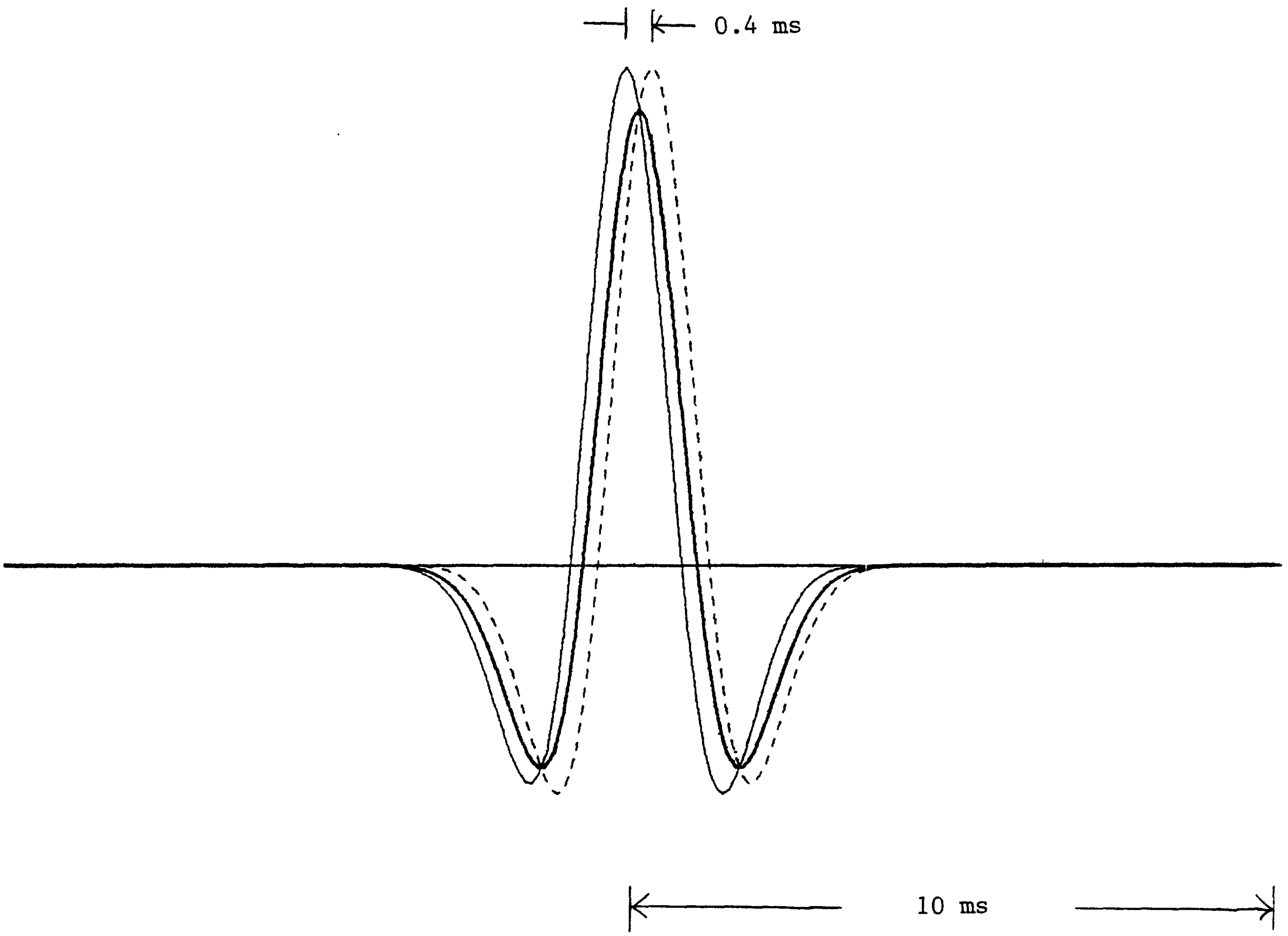

Figure 5.--Pressure response at $r = a$ for the incident P-wave with respect to the orientation of the detector with $\emptyset = 90^{\circ}$, $\alpha = 6{,}000$ m/s, $\alpha_f = 1{,}500$ m/s, $\rho/\rho_f = 2.5$, $a = 0.24$ m, and 250 Hz Ricker wavelet. Heavy solid line represents the pressure at $r = 0$; light solid line at $r = a$ and $\theta = 0^{\circ}$; light dotted line at $r = a$ and $\theta = 180^{\circ}$.

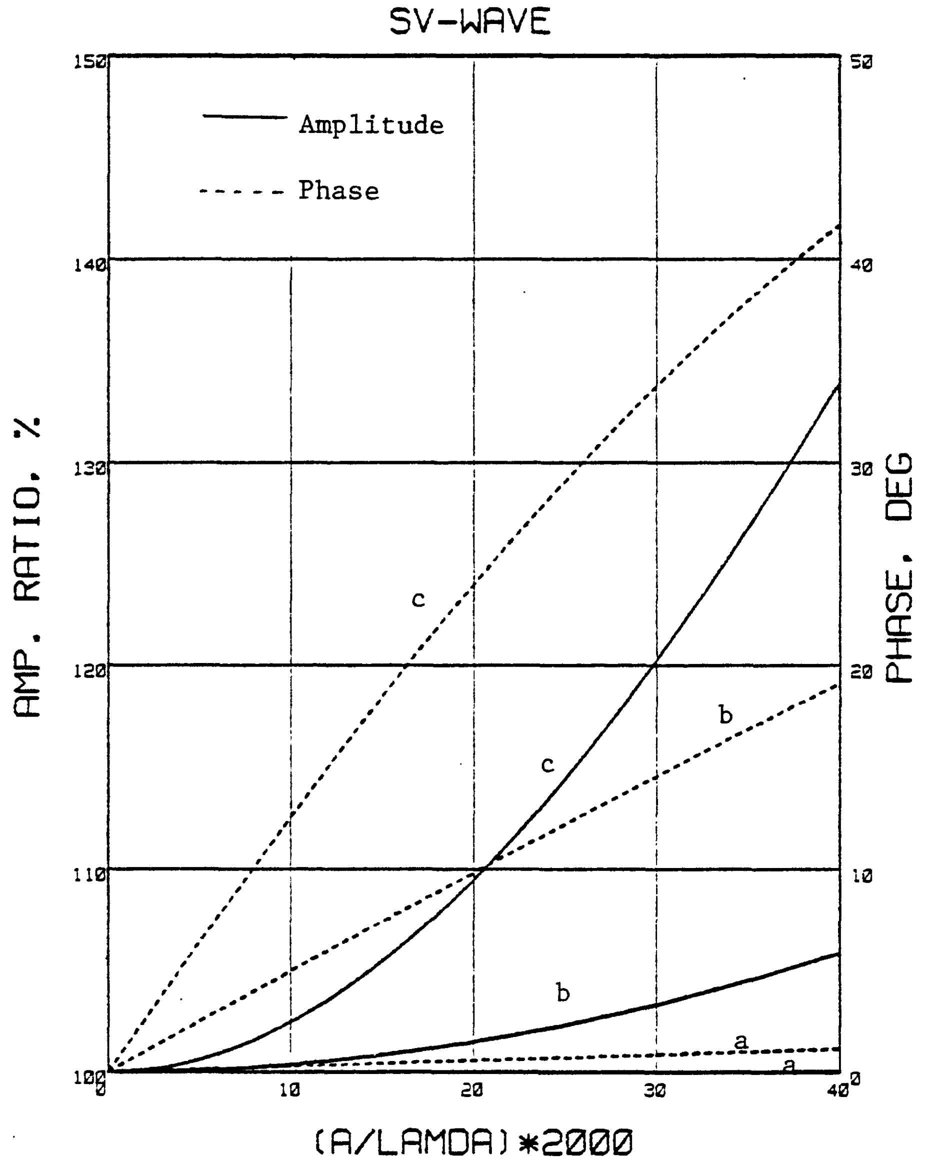

Figure 6.--Transfer function for the incident SV-wave with respect to the dimensionless parameter 2a/ and the formation of S-wave velocity with $\emptyset = 20^{o}$, $\theta = 0^{o}$, $r = a$, $\alpha_f = 1{,}500$ m/s, and $\rho/\rho_f = 2.5$
a) $\beta = 2{,}000/\sqrt{3}$ m/s; b) $\beta = 4{,}000/\sqrt{3}$ m/s; c) $\beta = 6{,}000/\sqrt{3}$ m/s.

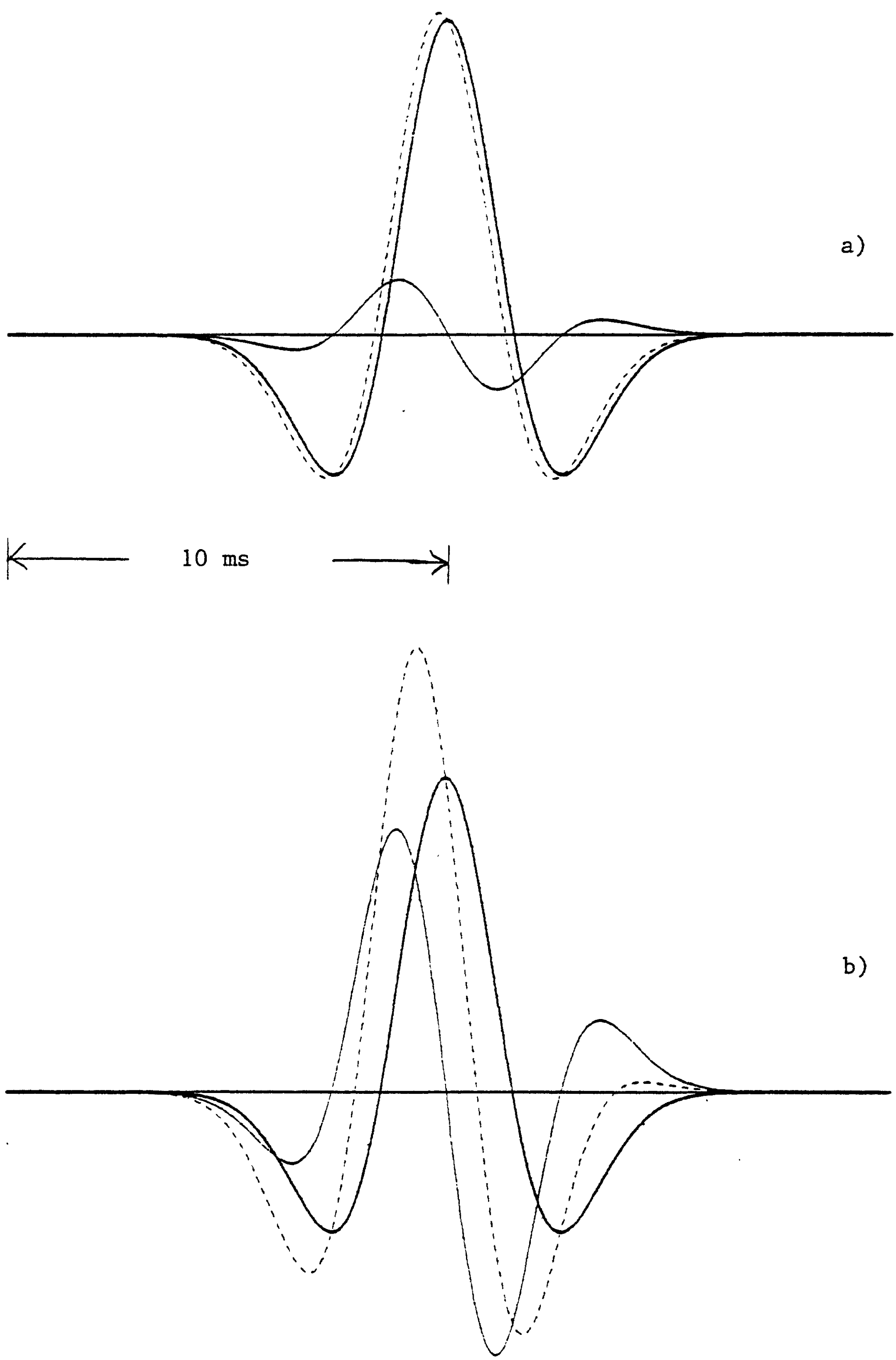

Figure 7.--Pressure response at $\theta = 0^{o}$ and r = a using 150 Hz Ricker wavelet for the incident SV-wave with respect to the formation S-wave velocity β with $\emptyset = 20^{o}$, α_f = 1,500 m/s, and ρ/ρ_f = 2.5. Heavy solid line represents the axis-symmetrical component; light solid line, the second-order component; light dotted line, the total pressure. a) $\beta = 4{,}000/\sqrt{3}$ m/s and a = 0.16 m; b) $\beta = 8{,}000/\sqrt{3}$ m/s and a = 1.32 m.

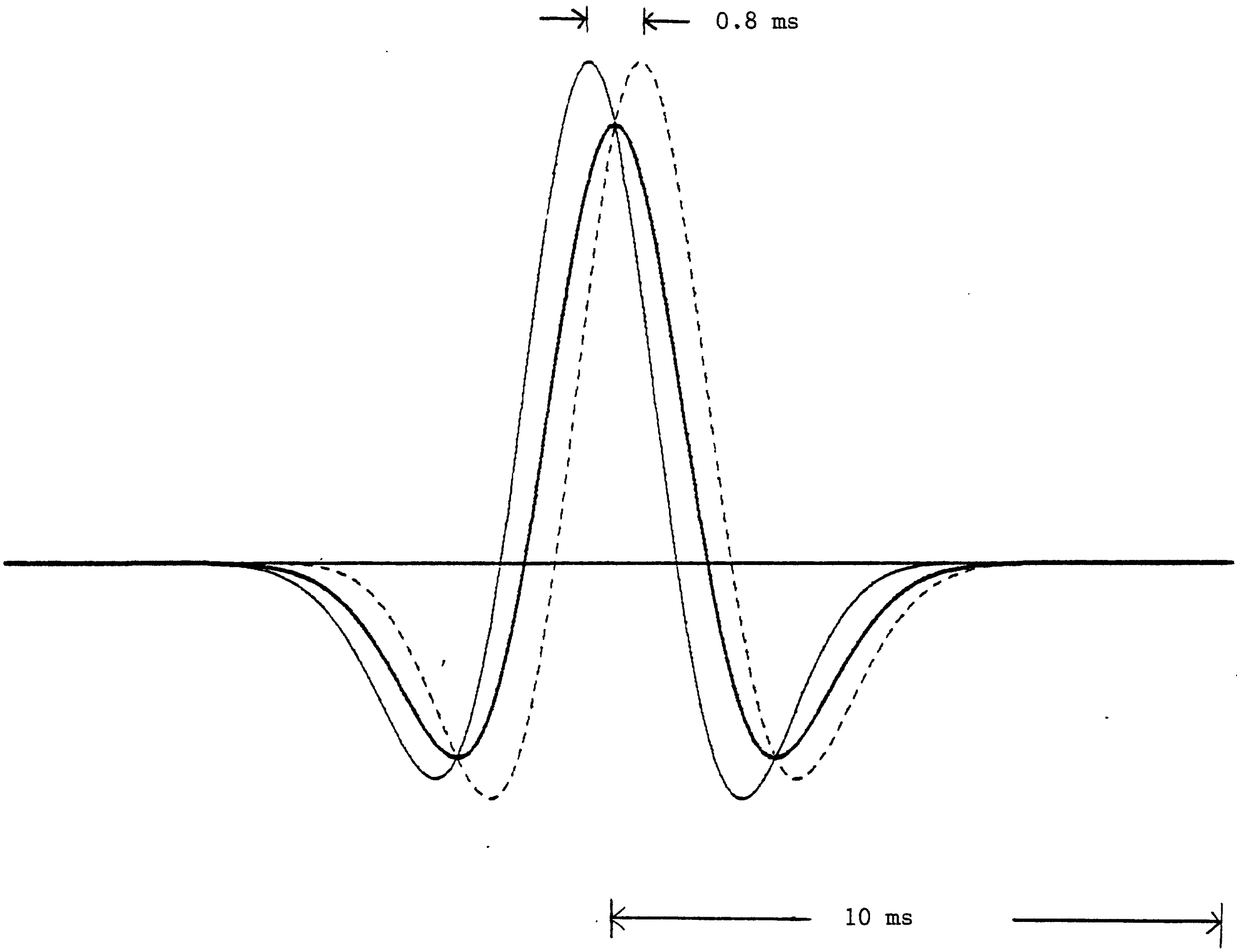

Figure 8.--Pressure response at r = a for the incident SV-wave with respect to the orientation of the detector with $\phi = 20^{\circ}$, $\beta = 6{,}000/\sqrt{3}$ m/s, α_f = 1,500 m/s, ρ/ρ_f = 2.5, a = 0.24 m, and 150 Hz Ricker wavelet. Heavy solid line represents the pressure at r = 0; light solid line at r = a and $\theta = 0^{\circ}$; light dotted line at r = a and $\theta = 180^{\circ}$.

APPENDIX

The radial displacements (U_r) at the wall of a fluid-filled borehole from incident plane wave (Lee, 1985a), are as follows.

A. Incident P-wave:

$$U_r = S(\omega)\cos\theta\sin\phi + S(\omega)\frac{i\omega a}{\alpha}\left[\frac{\alpha^2 T_\alpha (1-2\beta^2\cos^2\phi/\alpha^2)}{2\beta^2 (T_\alpha + \rho_f/\rho)} + \frac{\cos 2\theta \sin^2\phi}{(1-\beta^2/\alpha^2)}\right], \tag{A-1}$$

with

$$T_\alpha = \frac{\beta^2}{\alpha_f^2}\left(1 - \frac{\alpha_f^2\cos^2\phi}{\alpha^2}\right).$$

$S(\omega)$: displacement waveform of the incident wave.

B. Incident SV-wave:

$$U_r = S(\omega)\cos\theta\cos\phi + S(\omega)\frac{i\omega a}{\beta}\frac{\sin 2\phi}{2}\left[\frac{T_\beta}{(T_\beta + \rho_f/\rho)} + \frac{\cos 2\theta}{(1-\beta^2/\alpha^2)}\right], \tag{A-2}$$

with

$$T_\beta = \frac{\beta^2}{\alpha_f^2}\left(1 - \frac{\alpha_f^2 \cos^2\phi}{\beta^2}\right).$$

C. Incident SH-wave:

$$U_r = S(\omega)\sin\theta$$

$$+ S(\omega)\frac{i\omega a}{\beta}\,\frac{\sin 2\theta \sin\phi}{(1 - \beta^2/\alpha^2)}\,. \qquad \text{(A-3)}$$